Journal of Information Hiding and Multimedia Signal Processing ©2018 ISSN 2073-4212
Ubiquitous International Volume **9**, Number **3**, May **2018**

An Efficient Region-based Active Contour Method via Local Information for Image Segmentation

Xiao-Liang Jiang[1,2], Zhao-Zhong Zhou[1,*], Hui-Ling Geng[1],
Qi-Le Zhang[3], Zhong-Kui Dai[1] and Yuan-Xiang Zhang[1]

[1]College of Mechanical Engineering, Quzhou University, Quzhou, Zhejiang 324000, China

[2]College of Mechanical Engineering, Southwest Jiaotong University, Chengdu, Sichuan 610031, China

[3]Rehabilitation Department, Quzhou People's Hospital, Quzhou, Zhejiang 324000, China

[*]Corresponding Author:*zzz_2221@163.com*

Received December, 2017; revised March, 2018

Abstract. *Region-based active contour models are popular and often used to handle images with intensity inhomogeneity, but they may meet great difficulties when the intensity of the target and the background is similar. To solve this issue, a novel segmentation framework that considers the impact of local information is presented in this paper. In the proposed method, we incorporate the local information into region-scalable fitting (RSF) energy, which relies on local spatial and local gray level information simultaneously to improve the segmentation results. By using this local information, the new RSF model has edge identification ability and reducing the effect of noise. Then, a penalty term is incorporated into the modified energy functional to avoid the re-initialization. Finally, minimization of this energy function with a level set regularization term. A comparative performance evaluation is tested to demonstrate the superiority of the proposed method, showing higher robustness of noise and more efficient as compared with traditional algorithms.*

Keywords: Image segmentation, Active contour, RSF, Local information, Local spatial, Local gray level

1. **Introduction.** Image segmentation has always been an essential problem that divides the whole image into a finite number of distinct regions. So far, numerous good algorithms have been widely studied and used for different application [1-5]. Among the proposed segmentation methods, active contour models (ACM) [6-10] have become to be considerably effective and influential approaches. The basic idea of ACM is to partition the image by driving a curve to the desired contour based on an energy-minimizing algorithm. Generally speaking, most of active contour models can be classified into edge-based [11-13] and region-based [14-16]. Region-based method utilizing the statistical information, i.e. Chan Vese (C-V) model [17] performs better on images with weak edges. In order to obtain satisfied segmentation, C-V assumes that target and background in an image are statistically homogeneous so as to minimize a given energy functional. However, this model can't achieve good results for segmenting heterogeneous objects due to the lack of local statistical information.

Recently, many scholars have taken local intensity information into account. In [18], Li et al. presented a RSF active contour method, which utilizes the local intensity information efficiently. Therefore, that model is good at handling images with intensity non-uniformity. In [19], Wang et al. presented local Gaussian distribution fitting (LGDF)

energy with varying mean and variance to describe the image model. Thereby it can deal with targets with different grayscale variances. He et al. [20] presented an improved RSF algorithm based on local entropy, where the modified energy is redefined as a weighted energy that is come from the grayscale distribution of image. It is more flexible initialization and stronger anti-noise capability as compared with traditional RSF algorithms. Chen et al. [21] presented a region active contour method with global constraint that is constructed by a Gaussian Mixture Model. Under the joint action of local and global constraints, this model can achieve more efficient, more efficient, stable and precise results. Ding et al. [22] proposed a segmentation method based on optimized Laplacian of Gaussian energy, which can achieve superior segmentation performance in terms of visual perception and robustness.

In this paper, we propose a robust image segmentation method, called region-scalable fitting with local information (LIRSF). In order to evaluate the pixel similarity, we construct a novel RSF energy, which relies on local spatial and local gray level information simultaneously. Based on the weight function, our method could give a more accurate and less sensitive to initial contour. The rest of this paper is organized as follows. In Section 2, we briefly review some related works. In the next section, we concentrate on the whole framework of our method. In Section 4, experimental results will be described. Finally, we summarize our work in the last Section.

2. **Background.**

2.1. **RSF model.**

Li et al. [18] introduced a RSF active contour method, which specifies by a Gaussian kernel. For a given image $I : \Omega \subset R^2$, this RSF energy is given by:

$$\begin{aligned} E^{RSF}(C, f_1, f_2) = \lambda_1 \int_\Omega \int_{inside(C)} K_\sigma(x-y)|I(y) - f_1(x)|^2 dydx \\ + \lambda_2 \int_\Omega \int_{outside(C)} K_\sigma(x-y)|I(y) - f_2(x)|^2 dydx \end{aligned} \tag{1}$$

where $K_\sigma(x-y)$ is denotes a Gaussian kernel with standard deviation σ, λ_1 and λ_2 are nonnegative weighting coefficients, the parameters f_1 and f_2 are two values that approximate the image intensity $inside(C)$ and $outside(C)$. Although RSF model has show powerful capability with inhomogeneous intensity problem, it still relies on the initial curve placement and easy to fall into local minimum.

2.2. **LGDF model.**

In [19], Wang et al. presented a local Gaussian distribution fitting (LGDF) model which introduces grayscale variances information. By using maximum a posteriori probability and Bayes' rule, the energy can be formulated as:

$$E^{LGDF} = \int_\Omega \left(\sum_{i=1}^{2} \lambda_i \int_{\Omega_i} -\omega(x-y) \log p_{i,x}(I(y)) dy \right) dx \tag{2}$$

where $\omega(x-y)$ is a window function which satisfies $\omega(x-y) = 0$ for $|x-y| \geq \rho$ and $\int_{O_x} \omega(x-y)dy = 1$. The probability density $p_{i,x}(I(y))$ in region $O_x \bigcap O_i$ is defined by Gaussian distribution with mean $u_i(x)$ and variance $\sigma_i(x)$:

$$p_{i,x}(I(y)) = \frac{1}{\sqrt{2\pi}\sigma_i(x)} exp\left(-\frac{(u_i(x) - I(y))^2}{2\sigma_i^2(x)} \right), i = 1, 2 \tag{3}$$

Because of using local grayscale and local variance information, LGDF can segment regions with similar intensity means but different variances. However, this method still has the shortcoming that it is sensitive to the initial contour and the convergence rate is slow.

3. **The Proposed Method.**

3.1. **Energy functional of LIRSF model.** In this section, we present a new segmentation framework that takes both local spatial and local gray level information. Let $I : \Omega \subset R^2$ be the image domain, $\Omega \subset R^2$ is a given image, C be a closed curve which divides Ω into $\Omega_1 = inside(C)$ and $\Omega_2 = outside(C)$. So, the energy function can be defined:

$$\begin{aligned} E^{LIRSF}(C, f_1, f_2) = \lambda_1 \int_\Omega W_{xy}(\int_{inside(C)} K_\sigma(x-y)|I(y) - f_1(x)|^2 dy)dx \\ + \lambda_2 \int_\Omega W_{xy}(\int_{outside(C)} K_\sigma(x-y)|I(y) - f_2(x)|^2 dy)dx \end{aligned} \tag{4}$$

Here, the weight W_{xy} composes of two parts: local spatial and local gray level information. It can be written as:

$$W_{xy} = W^s_{xy} * W^g_{xy} \tag{5}$$

For each pixel, the local spatial information indicates the damping range between the neighbor pixels and the central pixel, so it is given by

$$W^s_{xy} = exp\left(-\frac{max(|p(x) - p(y)|, |q(x) - q(y)|)}{\lambda_s}\right) \tag{6}$$

where λ_s is a scale parameter and the term $(p(x), q(x))$ denotes the spatial coordinate. From Eq. (6), we can estimate that the spatial information makes the effect of the pixels in local window change flexibly, and so that more local information is incorporated into our model. The local gray level information is given by

$$W^g_{xy} = exp\left(\frac{-\parallel I(x) - I(y) \parallel^2}{\lambda_g \times \sigma^2_{g\_x}}\right) \tag{7}$$

where the parameter λ_g is a scale factor, while σ_{g_x} is calculated as:

$$\sigma_{g\_x} = \sqrt{\frac{\sum_{y \in N_x} \parallel I(x) - I(y) \parallel^2}{N_R}} \tag{8}$$

where $I(x)$ is gray value of the central pixel x with a spatial local window N_x and $I(y)$ is gray value of the yth pixles in local window, N_R denotes the cardinality of N_x ignoring the center pixel. Since the eight-neighbor pixel contain the dominant information of the central pixel, the size of N_x is set as 5×5. Eq. (7) indicates that when the intensity value $I(y)$ of the yth neighbors of central pixel x is close to $I(x)$, the value of denominator is small, W^g_{xy} should be large and vice versa. The value of W^g_{xy} can be changed with different gray values of the pixels over an image and thus it indicates the damping range in the intensity values.

3.2. **Level set framework.** Let $\Omega \subset R^2$ be a two dimensional image space, and $I : \Omega \subset R^2$ be a given gray image. We assume that the image domain can be partitioned into two regions. These two regions can be represented as the regions outside and inside the zero level ϕ, that is $\Omega_1 = \{\phi > 0\}$ and $\Omega_2 = \{\phi < 0\}$. Therefore, the energy (4) can be

expressed as:

$$E^{LIRSF}(\phi, f_1, f_2) = \lambda_1 \int_\Omega W_{xy}(\int_{inside(C)} K_\sigma(x-y)|I(y)-f_1(x)|^2 H_\varepsilon(\phi(y))dy)dx + \lambda_2 \int_\Omega W_{xy}(\int_{outside(C)} K_\sigma(x-y)|I(y)-f_2(x)|^2(1-H_\varepsilon(\phi(y)))dy)dx \tag{9}$$

To smooth the zero level set, a length term is used to derive the contour during evolution, which is shown in Eq. (10). Furthermore, a penalty term presented by Li [23] is added to our method, it is given in Eq. (11).

$$L(\phi) = \int_\Omega (|\nabla H_\varepsilon(\phi(x))|)dx \tag{10}$$

$$P(\phi) = \int_\Omega \frac{1}{2}(|\nabla\phi(x)|-1)^2 dx \tag{11}$$

Therefore the entire energy functional is

$$F^{LIRSF}(\phi, f_1, f_2) = \lambda_1 \int_\Omega W_{xy}(\int_{inside(C)} K_\sigma(x-y)|I(y)-f_1(x)|^2 H_\varepsilon(\phi(y))dy)dx + \lambda_2 \int_\Omega W_{xy}(\int_{outside(C)} K_\sigma(x-y)|I(y)-f_2(x)|^2(1-H_\varepsilon(\phi(y)))dy)dx + \nu L(\phi) + \mu P(\phi) \tag{12}$$

where ν and μ are two positive constants.

3.3. **Energy minimization.** We minimize the energy $F^{LIRSF}(\phi, f_1, f_2)$ by utilizing the variational and gradient descent method. First, for fixed ϕ, minimization of $F^{LIRSF}(\phi, f_1, f_2)$ with respect to $f_i (i = 1, 2)$ satisfies the following equations:

$$\int_\Omega K_\sigma(x-y)|I(y)-f_i(x)|M_i(\phi(y)))dy = 0 \tag{13}$$

where $M_1(\phi)) = H_\varepsilon(\phi)$ and $M_2(\phi)) = 1 - H_\varepsilon(\phi)$. From Eq. (13), it can be easily obtained that

$$f_i(x) = \frac{\int_\Omega K_\sigma(x-y)I(y)M_i(\phi(y))dy}{\int_\Omega K_\sigma(x-y)M_i(\phi(y))dy} \tag{14}$$

For ϕ, we should fix f_1, f_2 and use stand gradient descent method to minimize the functional $F^{LIRSF}(\phi, f_1, f_2)$:

$$\frac{\partial\phi}{\partial t} = -\frac{\partial F}{\partial\phi} \tag{15}$$

By calculating this Gateaux derivative of energy function F^{LIRSF}, we have beginequation beginequation

$$\frac{\partial\phi}{\partial t} = -\delta_\varepsilon(\phi)(\lambda_1 e_1 - \lambda_2 e_2) + \nu\delta_\varepsilon(\phi)div(\frac{\Delta\phi}{|\Delta\phi|}) + \mu(\Delta\phi - div(\frac{\Delta\phi}{|\Delta\phi|})) \tag{16}$$

where

$$e_i(x) = \int_\Omega K_\sigma(x-y)W_{xy}|I(x)-f_i(y)|^2 dy, i = 1, 2 \tag{17}$$

$$H_\varepsilon(x) = \frac{1}{2}(1 + \frac{2}{\pi}\arctan(\frac{x}{\varepsilon})) \tag{18}$$

$$\delta_\varepsilon(x) = \frac{1}{\pi}\frac{\varepsilon}{\varepsilon^2 + x^2} \tag{19}$$

3.4. **Implementation.** The partial derivatives equation in the continuous domain defined in Eq. (16) can be handled by a finite difference method.

$$\phi_{i,j}^{k+1} = \phi_{i,j}^{k} + \Delta t \cdot L(\phi_{i,j}^{k}) \tag{20}$$

where $L(\phi_{i,j}^{k})$ is the approximation of the right hand side in Eq. (16) by the above spatial difference scheme. In our implementation, the level set functions can be simply initialized as a binary step function, which takes a negative constant value -2 inside the contour and a positive constant value 2 outside it. The main procedure of our new model is as follows:
Step 1: Input the original image $I(x)$.
Step 2: Compute the weight W_{xy} using Eq. (5).
Step 3: Initialize the level set function $\phi = \phi^0(x)$ to be a binary function:

$$\phi^0(x) = \begin{cases} -c_0, & x \quad is \quad inside \quad C \\ 0, & x \in C \\ c_0, & x \quad is \quad outside \quad C \end{cases} \tag{21}$$

Step 4: Initializing the parameters λ_s, λ_g, λ_1, λ_2, μ,ν, $\triangle t$, ε, σ.
Step 5: Update $e_1(x)$ and $e_2(x)$ using Eq. (17).
Step 6: Evolve level set function ϕ according to Eq. (16).
Step 7: Check whether the evolution is stationary. If not, return to step 5.

4. **Experimental Results.** In this subsection, RSF model [18], LCK model [24], LGDF model [19], LSD [25], NRBLSI model [26] and the proposed method are tested on images of various modalities. All of the experimental results are both obtained by the computer with Intel (R) Core (TM) i7-7700HQ @ 2.80 GHz CPU, 8 GB RAM and Windows 10 (64 bit) operating system. Unless otherwise stated, we set: $c_0 = 2.0$, time step $\Delta t = 0.1$, Gaussian kernel $\sigma = 3.0$, $\lambda_s = 3$, $\lambda_g = 0.5$, $\lambda_1 = 1.0$, $\lambda_2 = 1.0$, $\mu = 1.0$, $\varepsilon = 1.0$, $\nu = 0.001 * 255 * 255$.

4.1. **Segmentation of synthetic images.** Fig. 1 shows the results on four synthetic images with multiple levels of distinct intensities. The first column is the original images with their red initial contours. In the first two rows, the intensity of the target and the background are homogeneous. In the last two rows, the intensity of the background is homogeneous while the target is different. As shown in the fifth column of Fig. 1, LSD model is able to obtain the desired targets in the third and fourth images, but it is fallen into local minimum in the first two images. The segmentation results with other models proved that they have the capability of addressing images with multiple objects. In order to test the performance of our model, the computational time and iterations for segmentation are presented in Table 1. From the table we can see that LSD model yields the lowest time complexity for all images, while the segmentation results are not acceptable. By inducing the local information of image which is based on the local spatial factor and the local gray factor, the computational time and iteration number are reduced to a great extent.

In order to demonstrate the advantage of our model, we have tested these algorithms on images with Gaussian noise levels {0.1%, 0.2%, 0.3%, 0.4% and 0.5%}. As shown in Fig. 2, when the noise density is 0.1%, we observe that RSF, LGDF and LSD models are very sensitive to noise, while other models can obtain desired results. For quantitative comparisons with different methods, the root mean squared error (RMSE) [27] is used to

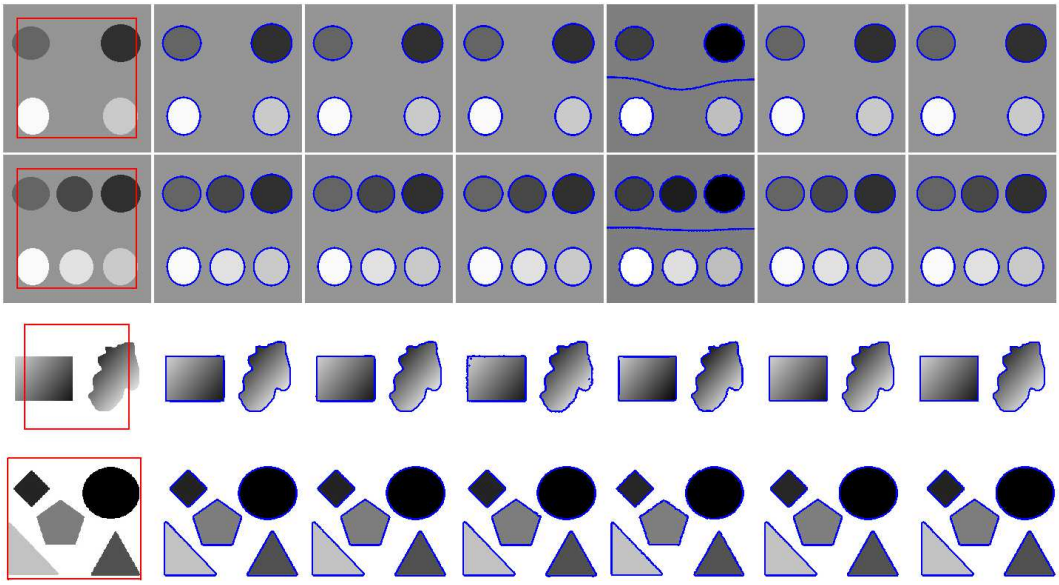

FIGURE 1. Experimental results on synthetic images with multiple levels of distinct intensities. The first column: the red initial contours. Second to last columns are the results obtained by RSF, LCK, LGDF, LSD, NRBLSI and our method.

TABLE 1. Comparison with iterations and computational time (s) for the images in Fig. 1.

	RSF		LCK		LGDF		LSD		NRBLSI		Our method	
	Iters	Time	Iters	Time	Iters	Time	Iters	Time	Iters	Time	Iters	Time
1	40	7.38	70	20.25	30	11.56	30	2.67	3	20.36	25	5.67
2	65	11.23	90	22.53	45	12.87	45	3.38	50	27.45	30	7.26
3	100	16.45	150	37.27	70	22.54	60	5.24	70	35.37	50	12.42
4	120	18.56	200	45.98	80	32.56	80	6.38	100	49.65	70	16.27

test the performance and the RMSE of these algorithms is given in Fig.3. From the results we can find that our algorithm has the best performance in terms of accuracy thanks to incorporating the local information when comparing with traditional active contour. This clearly shows that LIRSF model not only able to improve the segmenting accuracy, but also more robust for noisy.

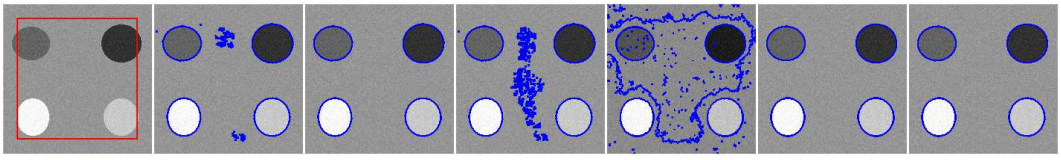

FIGURE 2. Experimental results on synthetic images corrupted by 0.1% Gaussian noise. The first column: the red initial contours. Second to last columns are the results obtained by RSF, LCK, LGDF, LSD, NRBLSI and our method.

4.2. **Experiments on medical images.** Next, we will show the experimental results performed on four typical medical images. In the first column of Fig. 4, there are four MR images and an ultrasound image. All of them are corrupted by obvious intensity inhomogeneity and high noise. As shown in Fig. 4, the first column is the original

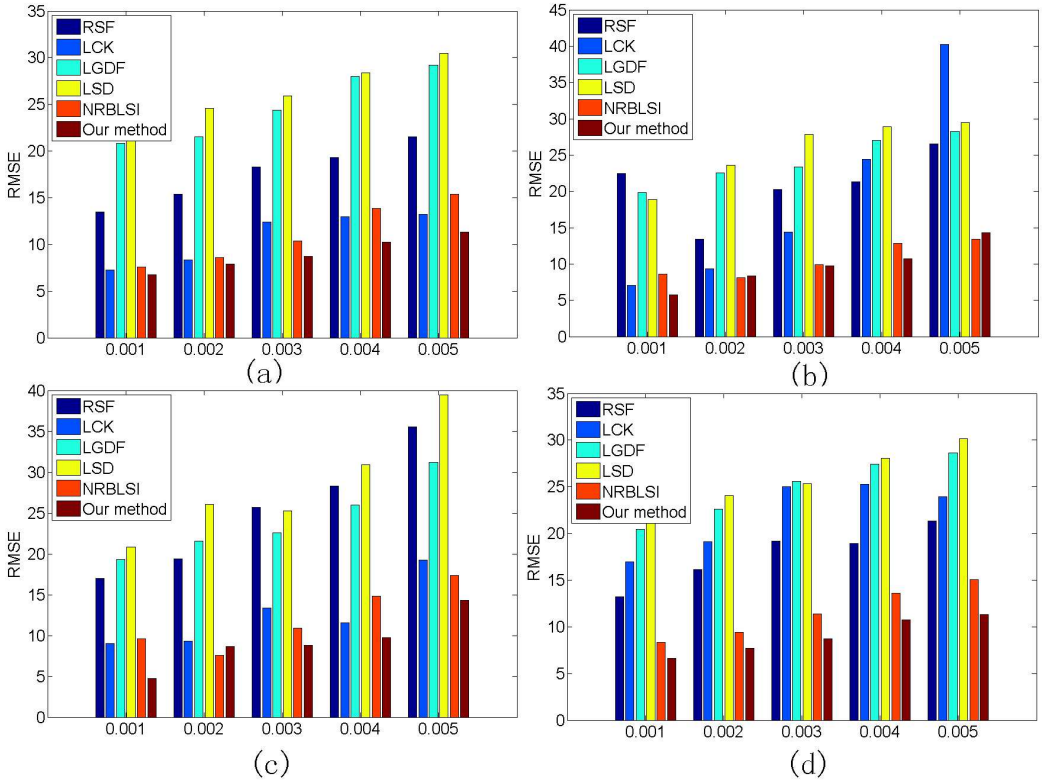

FIGURE 3. RMSE values obtaining by our method with different kinds of Gaussian noise in Fig. 1.

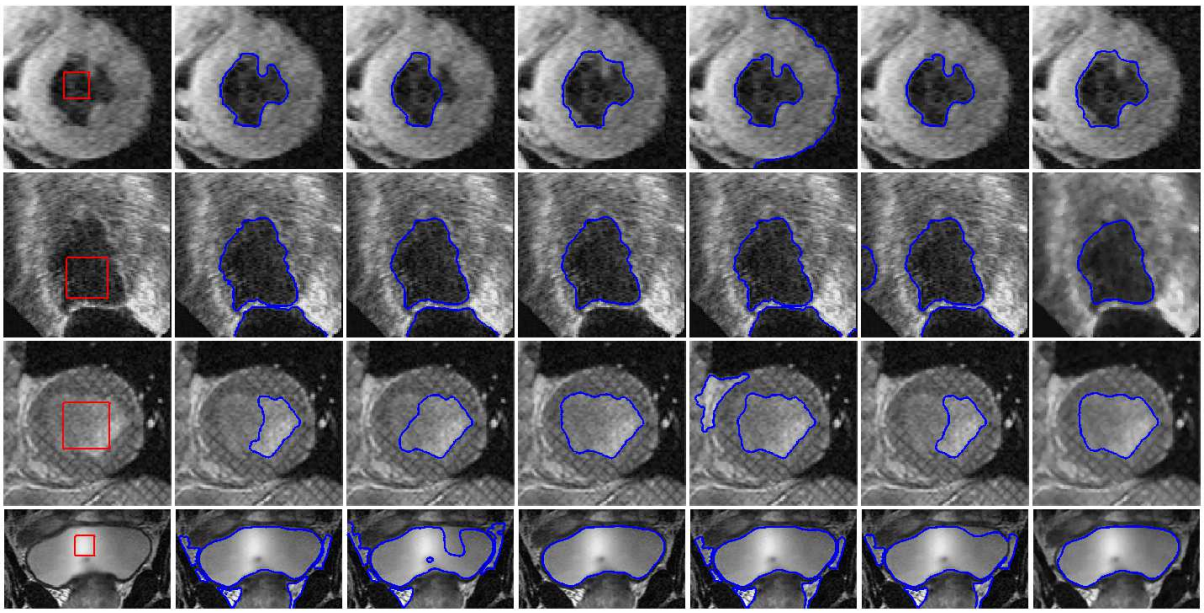

FIGURE 4. Experimental results on medical images. The first column: the red initial contours. Second to last columns are the results obtained by RSF, LCK, LGDF, LSD, NRBLSI and our method.(Image 1: $\nu = 0.001*255*255$; Image 2: $\nu = 0.06 * 255 * 255$; Image 3: $\nu = 0.05 * 255 * 255$; Image 4: $\nu = 0.03 * 255 * 255$; other setting: $\sigma = 5.0$)

image with red initial contour, and second to last columns show the segmentation results of RSF, LCK, LGDF, LSD, NRBLSI and our method. From the segmentation results, we can find that RSF, LCK, LSD and NRBLSI which use the Euclidean distance as a criterion of classification cannot detect the boundaries correctly. Taking more statistical characteristics into account, our method can obtain desirable results for medical images with intensity inhomogeneity.

4.3. **Robustness to initial contour.** Fig. 5 shows the segmentation results of our method to segment two real blood vessel images using six different initial contours. These images are corrupted by intensity inhomogeneity and strong noise in different levels. As shown in Fig. 5, the final segmentation results obtained after the convergence of these algorithms are marked as blue contours. Despite the great difference of these initial contours, our model can reach the desirable results in the proposed circumstances, which indicates that our method is robust to the initializations.

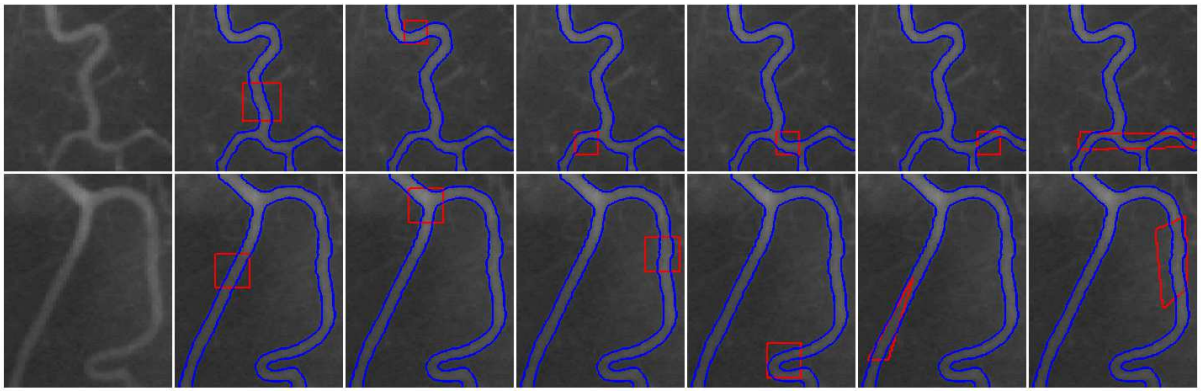

FIGURE 5. Results of our model on the real blood vessel image. The initial contours and the final contours are plotted as red contours and blue contours, respectively.($\nu = 0.0005 * 255 * 255$)

5. Conclusions.

In this paper, we propose a robust image segmentation method, which relies on local spatial and local gray level information simultaneously to improve the segmentation results. By using this local information, our method could give a more accurate and less sensitive to initial contour. As a result, the proposed method can achieve superior segmentation performance in terms of noise and intensity inhomogeneity. In addition, our model is more robust to initialization and slightly improves the accuracy of segmentation.

Acknowledgment.

The authors would like to thank the anonymous reviewers for their valuable comments and suggestions to improve this paper. Besides, this work is supported by the National Natural Science Foundation of China (No. 51275272, 51605252, 51605253), Zhejiang Provincial Natural Science Foundation of China (No. LQ17C160001, LQ18F010007), Key Laboratory of Air-driven Equipment Technology of Zhejiang Province(No.2018E10011).

REFERENCES

[1] Z. Ji, Y. Huang, Y. Xia, and Y. Zheng, A robust modified gaussian mixture model with rough set for image segmentation, *Neurocomputing*, vol. 266, no. C, pp. 550-565, 2017.

[2] J. Wen, J. Jiang, and Z. Yan, A new lattice boltzmann algorithm for assembling local statistical information with MR brain imaging segmentation applications, *Multidimensional Systems & Signal Processing*, vol.28, no. 4, pp. 1611-1627, 2017.
[3] A. Namburu, S. K. Samayamantula, and S. R. Edara, Generalised rough intuitionistic fuzzy c-means for magnetic resonance brain image segmentation, *IET Image Processing,* vol. 11, no. 9, pp. 777-785, 2017.
[4] F. Wang, Y. Wu, P. Zhang, Q. Zhang, and M. Li, Unsupervised sar image segmentation using ambiguity label information fusion in triplet Markov fields model, *IEEE Geoscience & Remote Sensing Letters*, vol. 14, no. 9, pp. 1479-1483, 2017.
[5] V. Rajinikanth, S. Satapathy, S. L. Fernandes, and S. Nachiappan, Entropy based segmentation of tumor from brain MR images a study with teaching learning based optimization, *Pattern Recognition Letters*, vol. 94, no. C, pp. 87-95, 2017.
[6] L. Wang, Y. Chang, H. Wang, Z. Wu, J. Pu, and X. Yang, An active contour model based on local fitted images for image segmentation, *Information Sciences*, vol. 418C419, pp. 61-73, 2017.
[7] B. Han, and Y. Wu, A novel active contour model based on modified symmetric cross entropy for remote sensing river image segmentation, *Pattern Recognition*, vol. 67, pp. 396-409, 2017.
[8] Y. T. Chen, A novel approach to segmentation and measurement of medical image using level set methods, *Magnetic Resonance Imaging*, vol. 39, pp. 175-193, 2017.
[9] R. Rouhi, and M. Jafari, Classification of benign and malignant breast tumors based on hybrid level set segmentation, *Expert Systems with Applications*, vol. 46, no. C, pp. 45-59, 2016.
[10] Z. Ren, Adaptive active contour model driven by fractional order fitting energy, *Signal Processing*, vol. 117, no. C, pp. 138-150, 2015.
[11] A. Pratondo, C. K. Chui, and S. H. Ong, Robust edge-stop functions for edge-based active contour models in medical image segmentation, *IEEE Signal Processing Letters,* vol. 23, no. 2, pp. 222-226, 2016.
[12] S. S. Suganthi, and S. Ramakrishnan, Anisotropic diffusion filter based edge enhancement for segmentation of breast thermogram using level sets, *Biomedical Signal Processing and Control*, vol. 10, pp. 128-136, 2014.
[13] M. Ciecholewski, An edge-based active contour model using an inflation/deflation force with a damping coefficient, *Expert Systems with Applications*, vol. 44, no. C, pp. 22-36, 2016.
[14] Q. Ge, L. Xiao, H. Huang, and Z. H. Wei, An active contour model driven by anisotropic region fitting energy for image segmentation, *Digital Signal Processing*, vol. 23, no. 1, pp. 238-243, 2013.
[15] S. Niu, L. de Sisternes, Q. Chen, T. Leng, and D. L. Rubin, Automated geographic atrophy segmentation for SD-OCT images using region-based CV model via local similarity factor, *Biomedical optics express,* vol. 7, no. 2, pp. 581-600, 2016.
[16] H. Ali, N. Badshah, K. Chen, and G. A. Khan, A variational model with hybrid images data fitting energies for segmentation of images with intensity inhomogeneity, *Pattern Recognition*, vol. 51, no. C, pp. 27-42, 2016.
[17] T. F. Chan, and L. A. Vese, Active contours without edges, *IEEE Transactions on Image Processing*, vol. 10, no. 2, pp. 266-277, 2001.
[18] C. M. Li, C. Y. Kao, J. C. Gore, and Z. H. Ding, Minimization of region-scalable fitting energy for image segmentation, *IEEE Transactions on Image Processing*, vol. 17, pp. 1940C1949, 2008.
[19] L. Wang, L. He, A. Mishra, and C. M. Li, Active contours driven by local Gaussian distribution fitting energy, Signal Processing, vol. 89, pp. 2435C2447, 2009.
[20] C. He, Y. Wang, and Q. Chen, Active contours driven by weighted region-scalable fitting energy based on local entropy, *Signal Processing*, vol. 92 , no. 2, pp. 587C600, 2012.
[21] Y. Chen, X. Yue, R. Xu, H. Fujita, Region scalable active contour model with global constraint, Knowledge-Based Systems, vol.120, no. C, pp. 57-73,2016.
[22] K. Ding, L. Xiao, and G. Weng, Active contours driven by region-scalable fitting and optimized Laplacian of Gaussian energy for image segmentation, *Signal Processing*, vol. 134, pp. 224-233, 2017.
[23] C. Li, C. Xu, C. Gui, and M. D. Fox, Distance regularized level set evolution and its application to image segmentation, *IEEE Transactions on Image Processing,* vol. 9, no. 12, pp. 3243C3254, 2010.
[24] L. Wang, and C. Pan, Robust level set image segmentation via a local correntropy-based K-means clustering, Pattern Recognition, vol. 47, no. 5 , pp. 1917-1925, 2014.
[25] L. Wang, H. Wu and C. Pan, Region-based image segmentation with local signed difference energy, *Pattern Recognition Letter*, vol. 34, no. 6 , pp. 637C645, 2013.

[26] L. Li, L. Zeng, C. Qiu and L. Liu, Segmentation of computer tomography image using local robust statistics and region-scalable fitting, *Journal of X-Ray Science and Technology,* vol. 20, no. 3, pp. 255-267, 2012.

[27] J. Yuan, J. J. Wang, and L. P. Liu, Active contours driven by local intensity and local gradient fitting energies, *International Journal of Pattern Recognition and Artificial Intelligence*, vol. 28, no. 3, pp. 1455006 (19 pages), 2014.